

Orthogonal Soft Pruning for Efficient Class Unlearning

Qinghui Gong, Xue Yang*, Xiaohu Tang

School of Information Science and Technology, Southwest Jiaotong University

Abstract

Machine unlearning aims to selectively remove class-specific knowledge from pretrained neural networks to satisfy privacy regulations such as the GDPR. Existing methods typically face a trade-off between unlearning speed and preservation of predictive accuracy, often incurring either high computational overhead or significant performance degradation on retained classes. In this paper, we propose a novel class-aware soft pruning framework leveraging orthogonal convolutional kernel regularization to achieve rapid and precise forgetting with millisecond-level response times. By enforcing orthogonality constraints during training, our method decorrelates convolutional filters and disentangles feature representations, while efficiently identifying class-specific channels through activation difference analysis. Extensive evaluations across multiple architectures and datasets demonstrate stable pruning with near-instant execution, complete forgetting of targeted classes, and minimal accuracy loss on retained data. Experiments on CIFAR-10, CIFAR-100, and TinyImageNet confirm that our approach substantially reduces membership inference attack risks and accelerates unlearning by orders of magnitude compared to state-of-the-art baselines. This framework provides an efficient, practical solution for real-time machine unlearning in Machine Learning as a Service (MLaaS) scenarios.

1 Introduction

As data-driven AI systems become integral in critical domains such as healthcare, finance, and autonomous driving, modern machine learning models increasingly depend on large-scale datasets containing sensitive, private, or copyright-protected information. In response, global privacy regulations—including the European GDPR [1], Luxembourg’s CNPD [2], California’s CCPA [3], and Brazil’s LGPD [4] have established the “right to be forgotten” [5], empowering users to request deletion of their personal data and any derived model representations. This evolving legal landscape poses significant challenges in balancing privacy compliance with model utility.

Machine Learning as a Service (MLaaS) platforms [6–8] train models on data aggregated from diverse owners and provide inference under strict latency

constraints [9,10]. Simultaneously, data owners may issue unlearning requests to revoke consent, creating an inherent tension between timely inference and privacy compliance.

Existing machine unlearning methods largely treat unlearning and inference as separate, disjointed processes, which hampers real-time compliance in latency-sensitive MLaaS environments [11]. Efficiently removing the influence of target data without full retraining or excessive parameter storage, while preserving accuracy on retained data, remains an open and critical challenge.

Early approaches, such as fast retraining [12] and the SISA framework [13], provide exact unlearning but incur substantial computational and storage costs. To alleviate this, approximate methods manipulating model parameters have been proposed, including second-order parameter offset estimation via influence functions [14], parameter selection using Fisher information [15], noise injection with repair mechanisms [16], boundary projection [17], teacher-student distillation [18], and gradient-magnitude-based parameter selection [19]. These methods focus on fine-grained parameter updates but overlook the structured, block-wise nature of neural networks—such as channels or filters—limiting the efficiency and precision of class-specific unlearning.

More recently, adversarial example-based unlearning strategies have gained attention. For instance, Boundary Shifting (BS) [17] generates adversarial examples using the fast gradient sign method (FGSM) [20] and assigns new adversarial labels to the unlearning data, whereas Information Maximizing Unlearning (IMU) [21] leverages the stronger iterative projected gradient descent (PGD) [22] to produce adversarial samples. Although these approaches improve performance, they rely on external modules or offline pipelines, limiting their applicability in latency-sensitive scenarios.

In convolutional neural networks (CNNs), inter-filter correlations encode rich class-specific information. However, prevailing unlearning methods often manipulate isolated parameters or activations, leading to a disconnect between unlearning and inference that limits forgetting precision and real-time deployment. Figure 1 illustrates that discriminative filters in early convolutional layers exhibit significant activation differences between forgotten and retained classes, indicating strong class-specific coupling. Inspired by this, we propose the first convolutional kernel orthogonal-

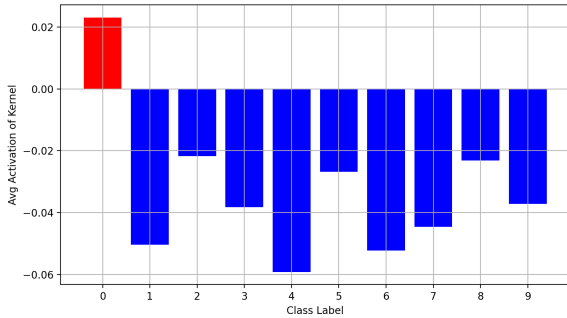
*Corresponding author.

ization method that explicitly enlarges the activation gap between forgotten and retained classes, effectively bridging unlearning and inference for real-time forgetting.

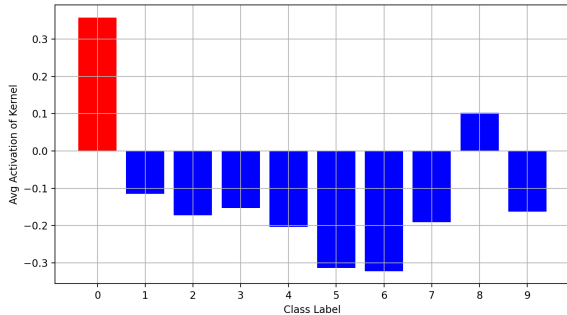
Our framework consists of: (1) Orthogonal Training, which reduces filter redundancy through decorrelation to enhance class discriminability; and (2) Dynamic Soft Pruning, which selectively suppresses filters correlated with target classes based on activation differences, achieving precise and stable class-specific forgetting while preserving overall model capacity.

Our main contributions are summarized as follows:

- A novel class-specific forgetting method: Combining orthogonality-based kernel analysis with dynamic soft pruning to precisely suppress filters tied to target classes for stable forgetting.
- Improved stability for retained classes: Orthogonality regularization strengthens discriminative features, reducing forgetting interference.
- Efficient, deployable pruning: A lightweight update enabling sub-second forgetting on standard MLaaS platforms, far faster than retraining or prior methods.



(a) Kernel 3 Activation



(b) Kernel 8 activation

Figure 1: Activation Differences of Top-2 Discriminative Kernels in Conv1: Forgotten (Red) vs. Retained (Blue)

2 Related Work

Research on machine unlearning can be broadly categorized into two directions: certified unlearning for convex and structured models, and approximate unlearning for deep neural networks.

2.1 Certified Unlearning for Structured Models

For models with tractable structure, a variety of methods provide theoretical guarantees for exact unlearning. Cao and Yang [12] introduced a statistical query framework that updates aggregated statistics to enable deletion without full retraining, though it relies on restrictive structural assumptions. Ginart et al. [23] formulated a probabilistic definition of approximate unlearning, ensuring the model output approximates that of a retrained counterpart without the target sample, primarily applicable to clustering tasks. Bourtole et al. [13] proposed the SISA framework, which partitions data and trains submodels independently, enabling low-cost partial retraining.

Other works focus on specific model classes. Guo et al. [24] developed certified unlearning techniques for linear regression. Neel et al. [25] applied projected gradient descent for data deletion in logistic regression. Brophy and Lowd [26] accelerated removal in random forests through node refreshing and cached statistics. Nguyen et al. [27] explored Bayesian posterior updates to support data removal. Although theoretically sound, these methods are largely restricted to simple or structured models and often require architectural modifications.

2.2 Approximate Unlearning for Deep Neural Networks

Due to the high dimensionality and non-convexity of deep networks, exact unlearning is typically infeasible. Instead, approximate strategies have been proposed to improve efficiency and scalability. Koh and Liang [14], and Golatkar et al. [15], utilized influence functions and Fisher information to identify sensitive parameters. Foster et al. [28] estimated weight importance using Fisher information and introduced synaptic dampening to suppress knowledge retention. Tarun et al. [16] combined noise injection with model repair mechanisms to mitigate memorized data.

Chen et al. [17] promote forgetting by generating adversarial examples using the fast gradient sign method (FGSM) [20] and assigning new adversarial labels, while Cha et al. [21] employ the stronger iterative projected gradient descent (PGD) [22] to produce adversarial samples for boundary projection. Chundawat et al. [18] proposed a student-teacher distillation framework that enforces forgetting through KL divergence. Fan et al. [19] pruned important gradients based on magnitude, while Wang et al. [29] removed class-discriminative channels using Term Frequency-Inverse Document Frequency, though without further analysis of inter-filter redundancy.

Our method enables fast, retrain-free, targeted unlearning by pruning class-specific channels via orthogonal kernel regularization—no extra models or adversarial steps needed. It’s lightweight, precise, and works across architectures with millisecond-level response.

3 Problem Definition

Consider a supervised learning setting with training dataset $D = \{(x_i, y_i)\}_{i=1}^N$, where inputs $x_i \in \mathbb{R}^d$ and labels $y_i \in \{1, \dots, C\}$. A deep neural network f is trained by minimizing a loss L :

$$f = \arg \min_f L(f, D), \quad (1)$$

to achieve high classification accuracy over all classes.

Given a subset of classes $U \subseteq \{1, \dots, C\}$ to be forgotten, the goal of unlearning is to modify f into an unlearned model f_u such that the information related to data $D_u = \{(x_i, y_i) \in D : y_i \in U\}$ is effectively removed, while preserving performance on the remaining data $D_r = D \setminus D_u$.

Formally, an unlearning algorithm A satisfies:

$$f_u = A(f, D, D_u), \quad (2)$$

and should meet the following objectives:

1. **Retention:** Maintain comparable accuracy on D_r , i.e.,

$$\mathbb{E}[L(f_u, D_r)] \approx \mathbb{E}[L(f, D_r)]. \quad (3)$$

2. **Forgetting:** The output distribution of f_u on D_u matches that of a model f_R trained exclusively on D_r , ensuring f_u behaves as if it never observed U :

$$P(f_u(x) = r) \approx P(f_R(x) = r), \quad \forall x \in D_u, \quad \forall r \in R, \quad (4)$$

where $R = \{1, \dots, C\} \setminus U$.

3. **Privacy:** The unlearned model f_u should not retain any information enabling membership inference attacks on D_u , i.e., the attack success rate should approach zero, indicating f_u behaves as if it never observed D_u .

$$\text{MIA}(f_u, D_u) \approx 0\%. \quad (5)$$

4. **Efficiency:** The computational cost of A is substantially lower than full retraining:

$$\text{Cost}(A) \ll \text{Cost}(\text{retraining } f). \quad (6)$$

4 Class Unlearning with Convolutional Kernel Orthogonality

Convolutional neural network channels often exhibit selective responsiveness to specific classes. Motivated by this, we are the first to combine convolutional kernel

orthogonal regularization with soft pruning in the context of class-level unlearning. Unlike previous orthogonal methods primarily aimed at improving training stability or reducing feature redundancy [30–32], our design focuses on achieving effective disentanglement and precise forgetting of class-specific features through the integration of orthogonal regularization and soft pruning.

The overall workflow of the proposed method is depicted in Figure 2, which outlines the key components and the orthogonality-driven unlearning mechanism.

4.1 Promoting Channel Independence via Orthogonality

To foster structural diversity and reduce representational redundancy within convolutional neural networks, we introduce an orthogonality-inducing regularization scheme aimed at promoting mutual independence among output channels. By encouraging orthogonal weight vectors across filters, the network is incentivized to allocate distinct subspaces to different channels, thereby enhancing its capacity to learn disentangled and class-discriminative features.

Let the weight tensor of the l -th convolutional layer be denoted as

$$W_l \in \mathbb{R}^{C_{\text{out}} \times C_{\text{in}} \times k \times k}, \quad (7)$$

where C_{in} and C_{out} correspond to the number of input and output channels respectively, and $k \times k$ represents the spatial extent of the convolutional kernel. To facilitate channel-wise orthogonality constraints, we first reshape the 4D kernel tensor into a 2D matrix representation by flattening each output filter into a row vector:

$$W_l^{(m)} \in \mathbb{R}^{C_{\text{out}} \times (C_{\text{in}} \cdot k^2)}. \quad (8)$$

Here, each row of $W_l^{(m)}$ corresponds to the vectorized weights of a single convolutional kernel. To enforce approximate pairwise orthogonality between these filters, we define the following regularization objective:

$$\mathcal{L}_{\text{ortho}} = \left\| W_l^{(m)} W_l^{(m)T} - I \right\|_F, \quad (9)$$

where I denotes the identity matrix of size $C_{\text{out}} \times C_{\text{out}}$, and $\|\cdot\|_F$ is the Frobenius norm, quantifying the deviation from perfect orthonormality. Minimizing $\mathcal{L}_{\text{ortho}}$ reduces inter-filter correlation, thereby promoting the disentanglement of learned representations.

The overall training objective integrates this orthogonality prior with the standard task-specific loss—e.g., cross-entropy—yielding the joint loss formulation:

$$\mathcal{L} = \mathcal{L}_{\text{CE}} + \lambda \mathcal{L}_{\text{ortho}}, \quad (10)$$

where $\lambda \in [0, 1)$ is a hyperparameter governing the trade-off between classification fidelity and channel independence. This formulation allows the model to simultaneously optimize for predictive performance and structural diversity in its internal feature space.

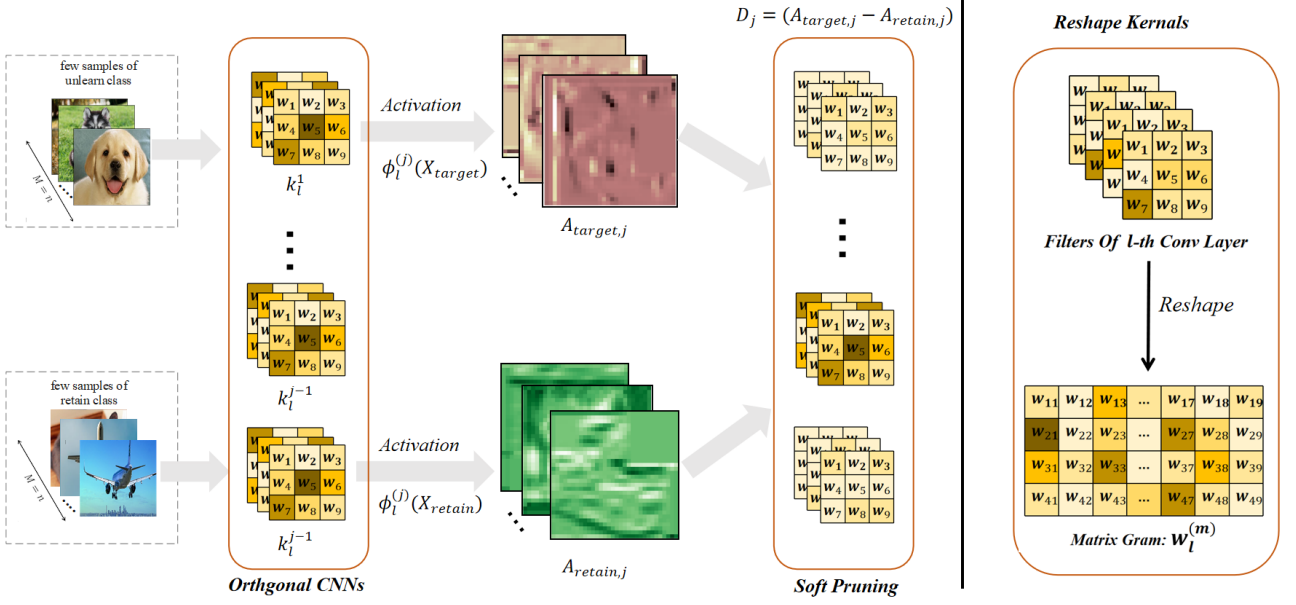


Figure 2: Overview of our class-aware pruning framework. Retained and forgotten data pass through a shared network to produce activation maps. Channel-wise discrepancy D_j quantifies class relevance and guides soft pruning of high-response filters.

As illustrated schematically in Figure 2, the orthogonality constraint operates on the reshaped kernel matrix (e.g., a transformation of four $3 \times 3 \times 1$ kernels into a 4×9 matrix), ensuring that each row occupies a unique direction in the embedding space. This design enforces an implicit regularization effect that enhances feature diversity, facilitates interpretability, and contributes to robustness under downstream pruning or forgetting tasks.

4.2 Identification of Class-Associated Channels

In response to a data deletion request targeting a specific class c_t , our objective is to selectively suppress the internal neural representations that predominantly contribute to the classification of c_t , while preserving the discriminative capacity of the model with respect to the remaining classes. To this end, we devise a quantitative criterion for identifying class-associated filters based on their activation patterns across class-partitioned datasets.

Concretely, for each convolutional layer l , we evaluate the class selectivity of its constituent filters by measuring their maximal activation responses when exposed to inputs belonging to the target class c_t and those from the complementary class set $\mathcal{C} \setminus \{c_t\}$. Let $\phi_l^{(j)}(X)_{u,v}$ denote the activation of the j -th filter at spatial location (u, v) in response to input X . The class-conditional average maximal activation of filter j is defined as follows:

$$A_{\text{target},j} = \mathbb{E}_{X \sim X_{\text{target}}} \left[\max_{u,v} \phi_l^{(j)}(X)_{u,v} \right], \quad (11)$$

$$A_{\text{retain},j} = \mathbb{E}_{X \sim X_{\text{retain}}} \left[\max_{u,v} \phi_l^{(j)}(X)_{u,v} \right], \quad (12)$$

where X_{target} and X_{retain} respectively denote the subsets of training data corresponding to class c_t and all other retained classes, and $\mathbb{E}[\cdot]$ denotes the expectation operator over the empirical data distribution.

The degree to which a filter is specialized for the target class is captured by the activation difference:

$$D_j = A_{\text{target},j} - A_{\text{retain},j}. \quad (13)$$

Intuitively, a large value of D_j suggests that filter j is preferentially activated by inputs from class c_t , and thus encodes information that is semantically aligned with this class. By ranking filters in descending order according to D_j , we prioritize those that exhibit the strongest class-specific activation patterns.

Let $\{D_{(1)}, D_{(2)}, \dots, D_{(C_{\text{out}})}\}$ denote the sorted activation differences such that

$$D_{(1)} \geq D_{(2)} \geq \dots \geq D_{(C_{\text{out}})}, \quad (14)$$

where C_{out} is the total number of output channels (filters) in layer l . Given a pruning ratio $r \in (0, 1]$, we define the pruned filter set \mathcal{P} as:

$$\mathcal{P} = \{j \mid D_j \geq D_{(\lceil r \cdot C_{\text{out}} \rceil)}\}. \quad (15)$$

This filter selection mechanism ensures that only the top- r fraction of filters with the strongest affinity to the target class are selected for pruning, thereby enabling targeted suppression of class-specific representations with minimal collateral degradation to non-target class performance.

Moreover, this criterion is layer-local and model-agnostic, and can be seamlessly integrated into convolutional backbones of varying depth and width, making it broadly applicable to diverse neural architectures.

4.3 Pruning and Fine-Tuning Strategy

To mitigate the influence of class-specific neural pathways while preserving discriminative capability on non-target classes, we propose a two-phase procedure integrating a soft filter suppression mechanism with an optional fine-tuning stage. This design facilitates gradual disentanglement of target-class dependencies, avoiding abrupt perturbations that may degrade generalization.

Empirically, a single application of this pruning strategy often suffices to achieve effective forgetting, thus rendering fine-tuning optional and applicable primarily in resource-abundant or high-accuracy-demand scenarios.

Soft Pruning with Rank-Adaptive Attenuation. Unlike hard pruning which irreversibly removes filter parameters, our soft pruning attenuates filter weights in a rank-aware manner. Let $\mathcal{P} = \{j_1, j_2, \dots, j_{N_p}\}$ be the set of filters selected for pruning in layer l , sorted such that $D_{j_1} \geq D_{j_2} \geq \dots \geq D_{j_{N_p}}$. The update rule for each filter $j_k \in \mathcal{P}$ is

$$W_l^{(j_k)} \leftarrow W_l^{(j_k)} \cdot (1 - S_k), \quad (16)$$

where the pruning strength S_k is defined as

$$S_k = \max\left(\lambda, 1 - \frac{k}{N_p}\right), \quad (17)$$

with $\lambda \in [0, 1]$ a minimum suppression factor preventing complete deactivation. This ensures a monotonically decreasing attenuation while retaining a residual gradient flow for recovery.

Optional Fine-Tuning for Refinement. Post-pruning, the model may undergo fine-tuning to realign parameters and reinforce class separability. Parameter updates follow

$$\theta^{(t+1)} = \theta^{(t)} - \eta_t \nabla_{\theta} \mathcal{L}(\theta^{(t)}), \quad (18)$$

where θ represents model parameters, $\mathcal{L}(\cdot)$ the supervised loss, and η_t the learning rate scheduled exponentially:

$$\eta_t = \eta_0 \alpha^t, \quad (19)$$

with initial rate $\eta_0 > 0$, decay $\alpha \in (0, 1)$, and epoch t . Fine-tuning terminates upon validation convergence or reaching a predefined iteration limit, balancing stability and overfitting prevention.

5 Experiment Results

5.1 Experimental Settings

Datasets and Architectures. We evaluate our method on three standard image classification benchmarks: CIFAR-10 [33], CIFAR-100 [33], and TinyImageNet [34], covering diverse granularity and complexity.

To demonstrate architecture generality, we conduct experiments on ResNet-18, ResNet-50 [35], and VGG-16 [36], representing models of varying depths and design principles.

Experiments run on a workstation with dual 14-core Intel Xeon CPUs, NVIDIA TITAN Xp GPU (12GB), Ubuntu 20.04, CUDA 11.7, and PyTorch 1.13.

5.2 Comparisons

We compare our method with four representative unlearning baselines proposed in recent years. First, Retraining is considered the gold standard: it retrains a new model from scratch using the remaining data after removing the target class. Although computationally expensive, it provides an upper bound on unlearning performance. Second, the TF-IDF-based channel pruning method identifies convolutional channels that are most discriminative for the target class using a TF-IDF-inspired metric, prunes them, and fine-tunes the model to recover accuracy [29]. Third, Error-Maximizing Noise Injection (EMNI) introduces adversarial noise to alter model weights, achieving strong forgetting effects. A subsequent repair step helps maintain overall performance, and the method works without access to the original training data [16]. Lastly, Selective Synaptic Dampening (SSD) estimates parameter importance using the Fisher information matrix and dampens sensitive parameters related to the forget set, enabling post hoc unlearning without full retraining [28].

5.3 Evaluation Metrics

We evaluate the effectiveness of unlearning techniques across three critical dimensions: model accuracy, privacy preservation, and computational efficiency.

1) Accuracy. Model accuracy is measured separately on two disjoint test subsets: the retained data T_{D_r} and the unlearned data T_{D_u} , denoted as $A_{T_{D_r}}$ and $A_{T_{D_u}}$, respectively. An ideal unlearning mechanism achieves a high accuracy on T_{D_r} , reflecting preservation of learned knowledge, while simultaneously reducing accuracy on T_{D_u} , indicating successful forgetting of the targeted information.

2) Privacy. To rigorously quantify privacy leakage, we employ a Membership Inference Attack (MIA) framework [37]. Specifically, a support vector machine (SVM) classifier [38] is trained on the confidence scores corresponding to the target class to discriminate whether samples belong to the unlearned subset. lower MIA attack accuracy signifies enhanced privacy guarantees by effectively obfuscating the presence of unlearned data within the training distribution.

3) Computational Efficiency. We measure the unlearning time as the wall-clock duration required to complete the unlearning procedure. Minimizing time is essential to ensure the method’s practicality and suitability for real-world deployment scenarios.

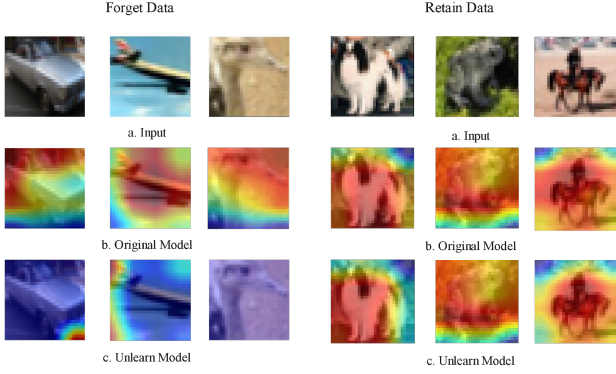


Figure 3: Grad-CAM heatmaps of ResNet50 on CIFAR10 before and after unlearning.

5.4 Main results

Impact of Orthogonal Regularization on Standard Training.

Although orthogonality constraints have previously been explored for improving training stability or representation diversity [30, 31], their compatibility with downstream unlearning tasks remains underexplored. In our context, orthogonality is introduced not for accuracy gains, but to promote channel independence and structural disentanglement that facilitate class forgetting.

To verify that this regularization does not hinder baseline performance, we conduct standard training with and without the orthogonal constraint. As shown in Table 1, the accuracy on both retained and unlearned classes remains comparable across datasets and architectures. In some cases, we even observe slight improvements in retained class performance. These results confirm that the proposed regularization can be seamlessly integrated into standard training workflows without sacrificing predictive performance while laying a solid foundation for downstream unlearning.

Dataset	Model	Orig.		Ortho.	
		$A_{Te_{Du}}$	$A_{Te_{Dr}}$	$A_{Te_{Du}}$	$A_{Te_{Dr}}$
CIFAR-10	ResNet-18	97.60%	93.13%	96.00%	94.13%
	ResNet-50	97.60%	94.02%	98.60%	95.31%
	VGG-16	97.80%	93.42%	97.80%	93.42%
CIFAR-100	ResNet-18	89.60%	78.03%	87.60%	77.28%
	ResNet-50	91.00%	81.22%	89.00%	80.56%
	VGG-16	84.00%	69.94%	85.00%	71.02%
TinyImgNet	ResNet-18	80.00%	64.83%	76.00%	64.94%
	ResNet-50	84.00%	65.67%	78.00%	65.18%
	VGG-16	80.00%	59.35%	78.00%	60.63%

Table 1: Classification accuracy before and after orthogonalization.

Trade-off-free Forgetting. As shown in Table 3a, the orthogonalized model consistently surpasses the original across pruning ratios ranging from 0.01 to 0.05. It drives the accuracy on the unlearned set (U-set) close to zero while retaining high performance on the

retained set (R-set). In contrast, the original model exhibits strong coupling between U-set and R-set accuracy, reflecting insufficient class separation due to shared kernel responses.

By enforcing orthogonality, our method promotes filter diversity and encourages inter-class feature disentanglement. At a pruning ratio of 0.05, for instance, the orthogonalized model achieves total forgetting with minimal degradation on the R-set, illustrating an improved trade-off frontier.

Activation map visualizations (Figure 1) reveal that first-layer filters respond differently to forgotten and retained classes, indicating disrupted feature extraction for the former. Moreover, heatmap comparisons on the same input image before and after pruning (Figure 3) show reduced focus on key regions for forgotten classes, while responses for retained classes remain stable. Together, these findings highlight the effectiveness of orthogonal regularization in enabling selective forgetting without compromising performance on retained data.

Privacy Protection and Resource Efficiency.

Privacy protection is a critical metric for evaluating unlearning methods. As shown in Table 2, our method achieves membership inference attack (MIA) values controlled within 10% across multiple datasets. Although not reaching the absolute minimum MIA values—those are achieved by TD-IDF and Retraining methods, whose extensive retraining on retained data can disrupt the original feature space and thus reduce MIA to near zero—they require significantly more computation time. Our MIA results notably outperform SSD and EMNI, which often exceed 10%, demonstrating stronger privacy erasure capability.

From the perspective of resource efficiency, methods like EMNI claim to provide privacy protection by storing and maintaining adversarial noise for each class during training. This approach incurs substantial storage and computational overhead that grows linearly with the number of classes, limiting adaptability and real-time applicability.

In contrast, our approach only requires a minimal number of original samples (usually 1 to 5, often from a single training batch) without the need for auxiliary data structures. This significantly reduces computational and storage demands while improving execution speed and flexibility. Therefore, our method strikes an effective balance between privacy protection and resource efficiency.

Computational Efficiency. We measure computational efficiency by the unlearning time. As shown in Table 2, our method completes the unlearning process within 0.1 to 0.6 seconds, significantly faster than existing baselines. This efficiency stems from not requiring access to the full training data or model retraining, but instead executing forgetting with a single forward pass, which greatly reduces computational overhead. Such characteristics make our approach well-suited for latency-sensitive and resource-constrained environments, such as online services and MLaaS platforms [6].

In contrast, retraining methods require thousands of

Model	Method	CIFAR-10				CIFAR-100				Tiny ImageNet			
		$At_{e_{D_u}}$	$At_{e_{D_r}}$	Time	MIA	$At_{e_{D_u}}$	$At_{e_{D_r}}$	Time	MIA	$At_{e_{D_u}}$	$At_{e_{D_r}}$	Time	MIA
Res-18	Retrain	0.00%	92.29%	4360.8s	0.0%	0.0%	78.17%	5557.26s	0.0%	0.0%	64.20%	15935.06s	0.0%
	SSD	4.37%	89.30%	21.60s	4.2%	1.70%	76.29%	21.38s	2.2%	0.0%	61.56%	136.77s	6.57%
	EMNI	9.76%	91.80%	322.02s	13.90%	4.98%	73.89%	335.40s	5.98%	3.8%	59.43%	348.42s	9.8%
	TD-IDF	0.00%	92.10%	872.75s	0.0%	0.0%	78.20%	1111.43s	0.0%	0.0%	63.98%	3187s	0.0%
	Ours	0.0%	90.34%	0.1254s	5.3%	0.0%	74.45%	0.0906s	2.1%	0.0%	63.11%	0.2244s	1.90%
Res-50	Retrain	0.00%	94.49%	10648.0s	0.0%	0.0%	80.49%	11473.13s	0.0%	0.0%	65.32%	23105.83s	0.0%
	SSD	1.7%	90.23%	76.56s	4.12%	5.62%	78.15%	74.42s	8.26%	0.00%	61.87%	480.06s	3.65%
	EMNI	2.1%	92.28%	784.75s	3.2%	5.0%	78.02%	795.32s	6.21%	4.2%	62.43%	800.26s	7.03%
	TD-IDF	0.00%	94.10%	2129.62s	0.0%	0.0%	80.32%	2214.60s	0.0%	0.0%	65.49%	4401.70s	0.0%
	Ours	0.00%	92.31%	0.6138s	5.25%	0.0%	79.23%	0.4165s	2.14%	0.0%	61.79%	0.4623s	4.0%
VGG-16	Retrain	0.00%	92.61%	3976.71s	0.0%	0.0%	69.48%	4407.80s	0.0%	0.0%	60.89%	10033.68s	0.0%
	SSD	0.00%	86.19%	13.83s	4.21%	0.0%	65.43%	13.72s	2.79%	0.00%	59.95%	61.48s	4.21%
	EMNI	2.4%	90.28%	289.81s	2.53%	3.2%	66.57%	300.53s	8.32%	2.8%	56.38%	312.63s	5.72%
	TD-IDF	0.0%	93.20%	994.09s	0.0%	0.0%	69.52%	1101.95s	0.0%	0.0%	60.79%	2509.17s	0.0%
	Ours	0.0%	88.64%	0.1472s	0.1%	0.0%	62.30%	0.1344s	9.68%	0.0%	57.24%	0.1051s	2.97%

Table 2: Comparison of unlearning performance across different methods and model architectures. All evaluations are performed by forgetting the first class in the dataset.

Pruning Ratio	Orthogonal Model		Original Model	
	$At_{e_{D_u}}$	$At_{e_{D_r}}$	$At_{e_{D_u}}$	$At_{e_{D_r}}$
0.01	78.70%	93.81%	92.40%	92.29%
0.02	42.00%	92.84%	84.35%	92.25%
0.03	16.10%	91.87%	76.40%	92.21%
0.04	1.7%	90.39%	68.30%	92.01%
0.05	0.0%	90.34%	43.30%	89.60%

(a) Effect of different pruning ratios r on forgetting performance.

Pruning Strength	Orthogonal Model	
	$At_{e_{D_u}}$	$At_{e_{D_r}}$
1.0	0.0%	66.47%
0.9	0.0%	71.09%
0.8	0.0%	80.27%
0.7	0.0%	81.96%
0.6	0.0%	84.96%
0.5	0.0%	85.27%
0.4	0.0%	90.34%
0.3	1.4%	90.53%
0.2	5.3%	91.67%

(b) Effect of different pruning strengths λ on forgetting performance.

Table 3: Impact of Pruning Ratio and Strength on Class-Specific Forgetting in ResNet18 on CIFAR-10.

seconds to fully retrain the model, making frequent unlearning impractical. The TD-IDF approach suffers from substantial model damage caused by pruning, necessitating computationally intensive feature space reconstruction and retrieval to restore performance, resulting in long and unstable runtimes. Although SSD employs soft pruning, it relies on multiple backward passes to estimate the Fisher information matrix, incurring high computational costs and unstable latency, especially for large-scale models and datasets.

Overall, our method strikes a favorable balance between unlearning effectiveness and computational efficiency, providing a practical and scalable solution for real-world applications.

Analysis of Soft Pruning Parameters: Ratio and Strength. Building on the optimal pruning ratio $r = 0.05$ identified in Table 3a, we further explore the impact of varying pruning strengths λ on the accuracy of unlearned and retained classes, as presented in Table 3b. Experiments conducted with ResNet-18 on CIFAR-10 demonstrate that pruning strength plays a critical role in balancing forgetting effectiveness and overall model performance.

At a moderate pruning strength (e.g., $\lambda = 0.4$), the accuracy on the unlearned class is suppressed close to 0%, while the accuracy on retained classes remains high, indicating an effective trade-off. However, stronger pruning (e.g., $\lambda = 1.0$) further decreases unlearned class accuracy but also degrades retained class performance, suggesting that excessively aggressive pruning may harm model utility.

For instance, in the CIFAR-100 experiment with ResNet-50, the pruning ratio r is as low as 0.02, indicating that only about 2 out of 100 convolutional kernels per layer are pruned. This example demonstrates that our approach requires minimal parameter changes while effectively forgetting targeted classes, emphasizing its efficiency and practical applicability.

6 Conclusion

We propose a novel class-aware soft pruning framework that exploits convolutional kernel orthogonality to efficiently erase specific class knowledge from deep neural networks. Our approach achieves effective forgetting with minimal performance degradation and high computational efficiency, providing a practical solution for real-time machine unlearning in MLaaS environments.

References

- [1] Paul Voigt and Axel Von dem Bussche. The eu general data protection regulation (gdpr). *A practical guide, 1st ed.*, Cham: Springer International Publishing, 10(3152676):10–5555, 2017.
- [2] Faustine Cachera and Astrid Wagner. La commission nationale pour la protection des données (luxembourg). *DPO news*, 25(5):19–22, 2023.
- [3] Rob Bonta. California consumer privacy act (ccpa). Retrieved from State of California Department of Justice: <https://oag.ca.gov/privacy/ccpa>, 2022.
- [4] Edna Dias Canedo, Anderson Jefferson Cerqueira, Rogério Machado Gravina, Vanessa Coelho Ribeiro, Renato Camões, Vinicius Eloy dos Reis, Fábio Lúcio Lopes de Mendonça, and Rafael T de Sousa Jr. Proposal of an implementation process for the brazilian general data protection law (lgpd). In *ICEIS (1)*, pages 19–30, 2021.
- [5] Alessandro Mantelero. The EU proposal for a general data protection regulation and the roots of the ‘right to be forgotten’. *Comput. Law Secur. Rev.*, 29(3):229–235, 2013.
- [6] Mauro Ribeiro, Katarina Grolinger, and Miriam A. M. Capretz. Mlaas: Machine learning as a service. In *14th IEEE International Conference on Machine Learning and Applications, ICMLA 2015, Miami, FL, USA, December 9-11, 2015*, pages 896–902, 2015.
- [7] Google Brain Team. Tensorflow serving for model deployment in production. <https://www.tensorflow.org/serving/>, 2018.
- [8] NVIDIA Corporation. Nvidia triton inference server. <https://github.com/triton-inference-server/server>, 2020.
- [9] Daniel Crankshaw, Xin Wang, Giulio Zhou, Michael J. Franklin, Joseph E. Gonzalez, and Ion Stoica. Clipper: A low-latency online prediction serving system. In *14th USENIX Symposium on Networked Systems Design and Implementation, NSDI 2017, Boston, MA, USA, March 27-29, 2017*, pages 613–627, 2017.
- [10] Arpan Gujarati, Reza Karimi, Safya Alzayat, Wei Hao, Antoine Kaufmann, Ymir Vigfusson, and Jonathan Mace. Serving dnns like clockwork: Performance predictability from the bottom up. In *14th USENIX Symposium on Operating Systems Design and Implementation, OSDI 2020, Virtual Event, November 4-6, 2020*, pages 443–462, 2020.
- [11] Yuke Hu, Jian Lou, Jiaqi Liu, Wangze Ni, Feng Lin, Zhan Qin, and Kui Ren. ERASER: machine unlearning in mlaas via an inference serving-aware approach. In *Proceedings of the 2024 on ACM SIGSAC Conference on Computer and Communications Security, CCS 2024, Salt Lake City, UT, USA, October 14-18, 2024*, pages 3883–3897, 2024.
- [12] Yinzhi Cao and Junfeng Yang. Towards making systems forget with machine unlearning. In *2015 IEEE Symposium on Security and Privacy, SP 2015, San Jose, CA, USA, May 17-21, 2015*, pages 463–480, 2015.
- [13] Lucas Bourtole, Varun Chandrasekaran, Christopher A. Choquette-Choo, Hengrui Jia, Adelin Travers, Baiwu Zhang, David Lie, and Nicolas Papernot. Machine unlearning. In *42nd IEEE Symposium on Security and Privacy, SP 2021, San Francisco, CA, USA, 24-27 May 2021*, pages 141–159, 2021.
- [14] Pang Wei Koh and Percy Liang. Understanding black-box predictions via influence functions. In *Proceedings of the 34th International Conference on Machine Learning, ICML 2017, Sydney, NSW, Australia, 6-11 August 2017*, pages 1885–1894, 2017.
- [15] Aditya Golatkar, Alessandro Achille, and Stefano Soatto. Eternal sunshine of the spotless net: Selective forgetting in deep networks. In *2020 IEEE/CVF Conference on Computer Vision and Pattern Recognition, CVPR 2020, Seattle, WA, USA, June 13-19, 2020*, pages 9301–9309, 2020.
- [16] Ayush K. Tarun, Vikram S. Chundawat, Murari Mandal, and Mohan S. Kankanhalli. Fast yet effective machine unlearning. *IEEE Trans. Neural Networks Learn. Syst.*, 35(9):13046–13055, 2024.
- [17] Min Chen, Weizhuo Gao, Gaoyang Liu, Kai Peng, and Chen Wang. Boundary unlearning: Rapid forgetting of deep networks via shifting the decision boundary. In *IEEE/CVF Conference on Computer Vision and Pattern Recognition, CVPR 2023, Vancouver, BC, Canada, June 17-24, 2023*, pages 7766–7775, 2023.
- [18] Vikram S. Chundawat, Ayush K. Tarun, Murari Mandal, and Mohan S. Kankanhalli. Can bad teaching induce forgetting? unlearning in deep networks using an incompetent teacher. In *Thirty-Seventh AAAI Conference on Artificial Intelligence, AAAI 2023, Thirty-Fifth Conference on Innovative Applications of Artificial Intelligence, IAAI 2023, Thirteenth Symposium on Educational Advances in Artificial Intelligence, EAAI 2023, Washington, DC, USA, February 7-14, 2023*, pages 7210–7217, 2023.
- [19] Chongyu Fan, Jiancheng Liu, Yihua Zhang, Eric Wong, Dennis Wei, and Sijia Liu. Salun: Empowering machine unlearning via gradient-based weight saliency in both image classification and generation. In *The Twelfth International Conference on Learning Representations, ICLR 2024, Vienna, Austria, May 7-11, 2024*, 2024.

- [20] Ian J. Goodfellow, Jonathon Shlens, and Christian Szegedy. Explaining and harnessing adversarial examples. In *3rd International Conference on Learning Representations, ICLR 2015, San Diego, CA, USA, May 7-9, 2015, Conference Track Proceedings*, 2015.
- [21] Sungmin Cha, Sungjun Cho, Dasol Hwang, Honglak Lee, Taesup Moon, and Moontae Lee. Learning to unlearn: Instance-wise unlearning for pre-trained classifiers. In *Thirty-Eighth AAAI Conference on Artificial Intelligence, AAAI 2024, Thirty-Sixth Conference on Innovative Applications of Artificial Intelligence, IAAI 2024, Fourteenth Symposium on Educational Advances in Artificial Intelligence, EAAI 2024, February 20-27, 2024, Vancouver, Canada*, pages 11186–11194, 2024.
- [22] Aleksander Madry, Aleksandar Makelov, Ludwig Schmidt, Dimitris Tsipras, and Adrian Vladu. Towards deep learning models resistant to adversarial attacks. In *6th International Conference on Learning Representations, ICLR 2018, Vancouver, BC, Canada, April 30 - May 3, 2018, Conference Track Proceedings*, 2018.
- [23] Antonio Ginart, Melody Y. Guan, Gregory Valiant, and James Zou. Making AI forget you: Data deletion in machine learning. In *Advances in Neural Information Processing Systems 32: Annual Conference on Neural Information Processing Systems 2019, NeurIPS 2019, December 8-14, 2019, Vancouver, BC, Canada*, pages 3513–3526, 2019.
- [24] Chuan Guo, Tom Goldstein, Awni Y. Hannun, and Laurens van der Maaten. Certified data removal from machine learning models. In *Proceedings of the 37th International Conference on Machine Learning, ICML 2020, 13-18 July 2020, Virtual Event*, pages 3832–3842, 2020.
- [25] Seth Neel, Aaron Roth, and Saeed Sharifi-Malvajerdi. Descent-to-delete: Gradient-based methods for machine unlearning. In *Algorithmic Learning Theory, 16-19 March 2021, Virtual Conference, Worldwide*, pages 931–962, 2021.
- [26] Jonathan Brophy and Daniel Lowd. Machine unlearning for random forests. In *Proceedings of the 38th International Conference on Machine Learning, ICML 2021, 18-24 July 2021, Virtual Event*, pages 1092–1104, 2021.
- [27] Thanh Tam Nguyen, Thanh Trung Huynh, Phi Le Nguyen, Alan Wee-Chung Liew, Hongzhi Yin, and Quoc Viet Hung Nguyen. A survey of machine unlearning. *CoRR*, abs/2209.02299, 2022.
- [28] Jack Foster, Stefan Schoepf, and Alexandra Brintrup. Fast machine unlearning without retraining through selective synaptic dampening. In *Thirty-Eighth AAAI Conference on Artificial Intelligence, AAAI 2024, Thirty-Sixth Conference on Innovative Applications of Artificial Intelligence, IAAI 2024, Fourteenth Symposium on Educational Advances in Artificial Intelligence, EAAI 2024, February 20-27, 2024, Vancouver, Canada*, pages 12043–12051, 2024.
- [29] Junxiao Wang, Song Guo, Xin Xie, and Heng Qi. Federated unlearning via class-discriminative pruning. In *WWW '22: The ACM Web Conference 2022, Virtual Event, Lyon, France, April 25 - 29, 2022*, pages 622–632, 2022.
- [30] Jiayun Wang, Yubei Chen, Rudransh Chakraborty, and Stella X. Yu. Orthogonal convolutional neural networks. In *2020 IEEE/CVF Conference on Computer Vision and Pattern Recognition, CVPR 2020, Seattle, WA, USA, June 13-19, 2020*, pages 11502–11512, 2020.
- [31] Di Xie, Jiang Xiong, and Shiliang Pu. All you need is beyond a good init: Exploring better solution for training extremely deep convolutional neural networks with orthonormality and modulation. In *2017 IEEE Conference on Computer Vision and Pattern Recognition, CVPR 2017, Honolulu, HI, USA, July 21-26, 2017*, pages 5075–5084, 2017.
- [32] Nitin Bansal, Xiaohan Chen, and Zhangyang Wang. Can we gain more from orthogonality regularizations in training deep networks? In *Advances in Neural Information Processing Systems 31: Annual Conference on Neural Information Processing Systems 2018, NeurIPS 2018, December 3-8, 2018, Montréal, Canada*, pages 4266–4276, 2018.
- [33] Alex Krizhevsky, Geoffrey Hinton, et al. Learning multiple layers of features from tiny images. 2009.
- [34] Zoheb Abai and Nishad Rajmalwar. Densenet models for tiny imagenet classification. *CoRR*, abs/1904.10429, 2019.
- [35] Kaiming He, Xiangyu Zhang, Shaoqing Ren, and Jian Sun. Deep residual learning for image recognition. In *2016 IEEE Conference on Computer Vision and Pattern Recognition, CVPR 2016, Las Vegas, NV, USA, June 27-30, 2016*, pages 770–778, 2016.
- [36] Karen Simonyan and Andrew Zisserman. Very deep convolutional networks for large-scale image recognition. In *3rd International Conference on Learning Representations, ICLR 2015, San Diego, CA, USA, May 7-9, 2015, Conference Track Proceedings*, 2015.
- [37] Liwei Song and Prateek Mittal. Systematic evaluation of privacy risks of machine learning models. In *30th USENIX Security Symposium, USENIX Security 2021, August 11-13, 2021*, pages 2615–2632, 2021.

- [38] Marti A. Hearst. Trends & controversies: Support vector machines. *IEEE Intell. Syst.*, 13(4):18–28, 1998.

A Additional Experimental Results on CIFAR-10

Since CIFAR-10 comprises only 10 classes, we performed experiments on all classes to thoroughly validate the efficacy of our method. The results demonstrate that although OMP pruning induces a slight degradation in accuracy, it already achieves satisfactory performance. Furthermore, with a brief fine-tuning period of only 3 to 5 epochs, the model’s accuracy is effectively restored to near its original level. This indicates that the proposed pruning and fine-tuning pipeline can efficiently recover model performance across all classes with minimal computational overhead.

Class	Raw Model		Pruned Model		Fine-tuned Model		Time
	$A_{Te_{D_u}}$	$A_{Te_{D_r}}$	$A_{Te_{D_u}}$	$A_{Te_{D_r}}$	$A_{Te_{D_u}}$	$A_{Te_{D_r}}$	
1	96.00%	94.13%	0.0%	90.34%	0.0%	92.47%	16.40s
2	92.20%	94.58%	0.0%	89.79%	0.0%	94.00%	15.61s
3	90.50%	94.77%	0.9%	90.38%	0.0%	95.27%	16.48s
4	94.60%	94.31%	0.8%	90.67%	0.0%	92.83%	16.30s
5	90.80%	94.73%	1.0%	93.17%	0.0%	93.77%	15.63s
6	95.60%	94.20%	0.0%	90.06%	0.0%	92.43%	16.26s
7	95.30%	94.23%	0.0%	88.30%	0.0%	93.00%	16.41s
8	96.90%	94.06%	0.3%	87.14%	0.0%	92.90%	15.93s
9	97.30%	94.01%	1.0%	88.64%	0.0%	92.46%	18.30s
0	94.20%	94.33%	0.0%	89.84%	0.0%	93.74%	18.76s

Table 4: Class-wise Accuracy of ResNet-18 on CIFAR-10 Along the Pruning and Fine-tuning Pipeline.

Class	Raw Model		Pruned Model		Fine-tuned Model		Time
	$A_{Te_{D_u}}$	$A_{Te_{D_r}}$	$A_{Te_{D_u}}$	$A_{Te_{D_r}}$	$A_{Te_{D_u}}$	$A_{Te_{D_r}}$	
1	98.60%	95.31%	0.0%	92.31%	0.0%	93.81%	44.15s
2	93.70%	95.86%	0.0%	91.04%	0.0%	94.13%	50.61s
3	89.20%	96.36%	0.0%	92.86%	0.0%	95.70%	51.69s
4	96.40%	95.56%	0.0%	92.70%	0.0%	94.32%	50.54s
5	92.70%	95.97%	0.0%	90.06%	0.0%	95.10%	45.13s
6	98.10%	95.37%	0.0%	90.91%	0.0%	93.73%	44.50s
7	97.10%	95.48%	0.0%	89.30%	0.0%	93.92%	50.76s
8	97.50%	95.43%	0.0%	87.84%	0.0%	94.17%	45.80s
9	97.20%	95.47%	0.0%	88.76%	0.0%	94.13%	40.91s
0	95.90%	95.61%	0.0%	90.20%	0.0%	94.30%	40.95s

Table 5: Class-wise Accuracy of ResNet-50 on CIFAR-10 Along the Pruning and Fine-tuning Pipeline.

Class	Raw Model		Pruned Model		Fine-tuned Model		Time
	$A_{Te_{D_u}}$	$A_{Te_{D_r}}$	$A_{Te_{D_u}}$	$A_{Te_{D_r}}$	$A_{Te_{D_u}}$	$A_{Te_{D_r}}$	
1	97.80%	93.42%	0.0%	88.64%	0.0%	92.10%	29.10s
2	90.80%	94.20%	1.8%	89.13%	0.0%	93.12%	30.15s
3	89.60%	94.33%	4.3%	87.60%	0.0%	94.78%	30.65s
4	94.60%	93.78%	0.0%	85.50%	0.0%	92.89%	29.50s
5	88.10%	94.50%	0.8%	87.16%	0.0%	94.03%	31.65s
6	95.30%	93.70%	0.0%	83.79%	0.0%	92.82%	31.45s
7	95.40%	93.69%	0.1%	84.11%	0.0%	92.72%	29.30s
8	96.50%	93.57%	0.5%	85.93%	0.0%	92.27%	32.45s
9	95.60%	93.67%	0.0%	83.60%	0.0%	92.32%	25.92s
0	94.90%	93.74%	0.0%	85.84%	0.0%	93.31%	25.89s

Table 6: Class-wise Accuracy of vgg-16 on CIFAR-10 Along the Pruning and Fine-tuning Pipeline.